Influence on permeability of the structural parameters of heterogeneous porous media

Laurence Le Coq

INFLUENCE ON PERMEABILITY OF THE STRUCTURAL PARAMETERS OF HETEROGENEOUS POROUS MEDIA

L. LE COQ

Ecole des Mines de Nantes – GEPEA UMR CNRS 6144, BP 20277, 44307 Nantes Cedex 3, France

ABSTRACT

Predicting the macroscopic properties of porous media used in treatment processes is a complex task regarding 3-D structures at micro-, meso- and macro-levels. Currently, information is scarce concerning the influence, at a microscopic level, of the 3-D structure of fibrous media on the physical laws governing their macroscopic behaviour. Nevertheless, the relationship between macroscopic properties (pressure drop, treatment efficiency) and microstructure can be assessed thanks to suitable structure modelling theories. In this context, the present study proposes and compares different methods (mercury porosimetry and image analysis) for the structure characterization at a microscopic level of filtering fibrous media, such as nonwoven and woven fabrics. The results obtained show a porous structure gradient in the thickness of the nonwoven media studied in terms of porosity, pore size and tortuosity factor. Moreover, the influence on structural parameters of media compression, when submitted to friction forces exerted by flow during filtration tests, is established. A model for the determination of multi-level pore size distributions from mercury porosimetry data is proposed. The "equivalent pore" model is used to estimate the tortuosity factor. The influence of measured structural parameters on fibrous media permeability is studied in a classical model for flow through fibrous media.

Keywords: Mercury porosimetry, image analysis, pore size, porosity, tortuosity

INTRODUCTION

Porous materials are widely used in treatment processes for removing pollution from air and water for environmental purposes or for fluid purification in industry. In most cases, arrangements of porous material present different levels of pore size from macropores, ranging from millimetres to micrometres, to micropores, which can include pore sizes from micrometres to nanometres according to the porous material considered. Macropores are formed by porous material units that are either packed in a reactor, constituting an unconsolidated porous medium, or bonded together in the form of a nonwoven or woven membrane (consolidated porous medium). Macropores are also called inter-pores as they are involved in inter-material porosity. Usually, meso- and micropores represent, respectively, the pores at the surface and inside porous material, thus they develop the intra-material porosity.

For treatment process optimization and design purposes, it is a complex task to consider the multi-levels of pore size for the estimation of process macroscopic behaviour with regard to flow, mass and thermal transfer. The state of the art concerning the influence of hierarchical porous material on the physical laws governing the process in which the porous structure is involved mostly deals with homogenization techniques [1,2].

In this context, an accurate characterization of structural parameters at the local level is of interest and some studies related to paper are available in the literature [3,4]. The present study deals with the characterization of the structural parameters of fibrous media exhibiting a pore size gradient in their thickness. The two characterization methods compared (mercury porosimetry [5] and image analysis [6]) are developed to obtain different information about the porous structure of eight papers made of a glass fibre blend. On the one hand, mercury porosimetry measures porosity and pore hydraulic diameter distribution at the different pore scales (macro- to micropore) and for different compression levels of the media. Moreover, the tortuosity factor in the thickness of the media is deduced from mercury porosimetry measurements thanks to the "equivalent pore" model [7]. On

the other hand, image analysis of media cross-sections is performed to determine porosity, mean pore size and tortuosity factors for different sub-layers of the media (upstream, centre and downstream layers) [6]. From structural parameter data, permeability coefficients are calculated and compared with those deduced from permeametry measurements.

MATERIALS AND METHODS

Materials

Operating conditions of fibrous media production

Eight glass fibre nonwovens made by a papermaking process were studied. Fibrous media are mixtures of Glass Fibres (GF) of various diameters and lengths fabricated by using a standard hand sheet machine [8]. Three grades of glass fibre were used in this study corresponding to mean diameters (d) of 0.6, 2.7 and 6 μm, for fibre lengths (L) ranging between 500 d < L < 4000 d. The fibre composition of each medium is expressed considering the weight percentage of each fibre grade dispersed in the fibrous admixture.

Stock glass fibres were dispersed in water at an acidic pH of 2.5, at a concentration of 10 g l^{-1} using a propeller mixer. The dispersion operation was performed at 2500 to 3000 rd min^{-1} for 10 to 40 min according to fibre diameter and length, to avoid flocking of fibre. The required energy for a good dispersion increases with the length-to-diameter ratio for fibres of diameter greater than 1 μm [9]. For fibres of diameter less than 1 μm, the required energy increases with decreasing diameter. The acidic pH of the suspension improves fibre repelling [10].

The fibrous suspension was diluted in the mixing vessel of the hand sheet machine at a concentration of 0.5 g l^{-1} and mixed with a chemical binder (5 to 10 % in weight) for 30 s. The binder ensures the mechanical cohesion of the fibrous web. The suspension was then percolated through a forming fabric thanks to a suction system providing a vacuum pressure of 0.1 10^5 Pa. The fibrous mat obtained was drained for 0.5 to 4 min according to mat permeability and was slightly pressed (2000 Pa) onto blotting paper. A drying operation at 110 °C for 35 min produces strengthened fibrous media.

Considering the process used to make paper prototypes, the fibrous media obtained can be considered isotropic in the sheet plane but anisotropic in the thickness because of a fibrous composition gradient due to filtration on the forming fabric.

Fibrous media obtained

In order to study the influence of fibre diameter and length for media made of one or two grades of fibre, eight fibrous compositions were made. Four media were made of one fibre grade of mean diameter 0.6 or 2.7 μm. For the fibrous composition *100% 2.7*, three different media were produced according to fibre length: the first *100% 2.7* medium contained all the lengths of the fibre furnished, the second one was made only of the short fibres furnished corresponding to a mean length of 0.3 mm, and the third one was composed of long 2.7 μm fibres (mean length of 0.9 mm). The other four media were composed of a binary mixture of fibre grades 0.6 and 2.7 μm, or 0.6 and 6 μm. The textural and mechanical parameters of the eight prototype media are presented in Table 1.

Specific weight was approximately 75 g m^{-2} for all the media except the *67% 0.6 + 33% 2.7* prototype, which has a specific weight of 35 g m^{-2}. The body of paper, defined as the ratio of specific weight to thickness, represents the apparent density of the fibrous media. Table 1 shows no significant variation in body values with changes in fibre diameter. Nevertheless, considering the three *100% 2.7* media of different fibre length, body values seem to increase with decreasing fibre length. This indicates that longer fibres are favourable for a bulk porous structure. Lastly, tensile strength values are encouraging for fibrous media implementation in filtering systems.

Table 1. Textural and mechanical parameters of prototype media.

Media composition	Specific weight (g m^{-2})	e (μm)	Body $.10^6$ (g m^{-3})	Binder retained (%)	Tensile strength (N)
100% 0.6	75	350	0.21	5.1	/
33% 0.6 + 67% 2.7	76	377	0.20	4.5	21.7
100% 2.7 furnished	80	430	0.19	8.0	15.0
100% 2.7 – L=0.3 mm	85	356	0.24	8.8	15.2
100% 2.7 – L=0.9 mm	75	440	0.17	9.3	18.4
67% 0.6 + 33% 6	36	170	0.21	5.1	9.7
50% 0.6 + 50% 6	71	316	0.22	11.2	15.4
33% 0.6 + 67% 6	74	350	0.21	11.5	15.3

Characterization of Structural Parameters

The structure of porous media can be characterized considering two scalar quantities, porosity and pore hydraulic diameter, and a vector quantity, the tortuosity factor [4,11]. In the present study, tortuosity is characterized according to the mean flow path direction, that is to say according to medium thickness.

The mean pore hydraulic diameter ($<\phi>$) is defined as the ratio of the pore volume where fluid flows to the pore surface wetted by this fluid. It is commonly used to represent the characteristic dimension of a non-circular channel.

$$<\phi> = 4\,\frac{\varepsilon}{S_v} \qquad \text{(i)}$$

where S_v (m^{-1}) is the volume specific surface area of pores, which can be calculated as:

$$S_v = (1-\varepsilon)\frac{\text{fibre surface}}{\text{fibre volume}} \qquad \text{(ii)}$$

Two methods were developed to determine these structural parameters. The first one is based on post-processing of mercury porosimetry results. This technique gives access to the structural parameters of the overall medium at different levels of compression. The second method is based on stereological analysis of images obtained from media cross-sections and can characterize local structural parameters [12]. Indeed, in the case of heterogeneous or anisotropic porous media for environmental engineering processes, considering the overall structural parameters could lead to design errors or to deficient treatment performances. So, for particle filtration, an accurate prediction of fibrous media clogging can be achieved by considering the pore size gradient in the medium thickness.

Mercury porosimetry

Mercury porosimetry measurements were performed using a Micromeritics porometer (pore size range: 150 to 0.4 μm) on unstrained and compressed samples of the studied media. For each sample, three reproducibility experiments were performed. The mercury volume penetrating the porous medium was measured at different pressures so that a porosity versus pore size curve can be obtained according to the Washburn theory [13]. For data interpretation, a contact angle of 153 ° (glass – mercury) and a surface tension of 0.48 Nm^{-1} were considered.

The experimental data of porosity versus pore size were modelled considering the different levels of pore size distribution constituting a porous medium. In the case of the glass fibre prototypes, two levels of pore size can be distinguished: surface roughness and media internal pores. In the particular case of woven fabrics made of multi-fibre yarns, there are three levels of pore size: cloth surface roughness, inter-yarn pores due to yarn weaving and intra-yarn pores due to fibre twisting [14].

Considering the maximum porosity (ε_i^{max}) and the modal pore size (ϕ_i^{mod}) of each level (i) of pore size distribution, the following equation can be proposed to model the experimental probability distribution of porosity versus pore size:

$$\varepsilon(\phi_j) = P(\phi < \phi_j) = \sum_{i=1}^{k} \frac{\varepsilon_i^{max}}{\left[(\phi_j / \phi_i^{mod})^{\alpha_i} + 1\right]} \qquad \text{(iii)}$$

α_i is the slope attenuation coefficient at the inflection point of the cumulative porosity curve for the pore size distribution i. It is representative of how narrow a mono-modal distribution is: the smaller the α_i value, the narrower the pore size distribution.

Maximum porosity (ε_i^{max}), modal pore hydraulic diameter (ϕ_i^{mod}) and attenuation coefficient (α_i) are determined for each level (i) of pore size by an optimization algorithm. The iterative algorithm is based on a Newton method used to solve a least squares problem.

From the intrusion volume versus pore size data, a mercury saturation curve can be plotted considering, on the one hand, the dimensionless saturation (s) defined as the ratio between the cumulative mercury volume at a given pore size and the total incremental mercury volume and, on the other hand, the dimensionless hydraulic diameter (ϕ_0) equal to the ratio between the considered pore size and the modal pore size.

Silvy [7] models the porous structure using a homogenization approach that considers the pore/fibre interface at microscale as an ellipsoidal equivalent pore at macroscale characterized by its ellipticity coefficients b/a and c/a as well as by its surface area, equal to the measured pore/fibre interface at microscale. In order to estimate the flow through the homogenized porous model, he defines the flow direction that minimizes the pressure drops, as shown in Figure 1.

From the "equivalent pore" theory, the mercury saturation curve represents the progressive filling of the equivalent ellipsoid so as to maximize the hydraulic diameter at each step, as a result of the minimum loss of energy principle. In the case of a fibrous medium of isotropic structure in the paper plane and for c/a <1, the ellipticity coefficient (c/a) can be estimated by fitting the modelled saturation curve from equation (iv) with the experimental mercury saturation data.

$$\phi^{\circ} = \frac{3}{2}(1-s)^{2/3}\;\frac{1}{c/a}\;\frac{1+(c/a)^2\;\frac{1}{\sqrt{1-(c/a)^2}}\;\mathrm{Ln}\left[\frac{1}{c/a}\left(\sqrt{1-(c/a)^2}+1\right)\right]}{\sqrt{1+\left[\left(\frac{1}{c/a}\right)^2-1\right](1-s)^{2/3}}} \qquad \text{(iv)}$$

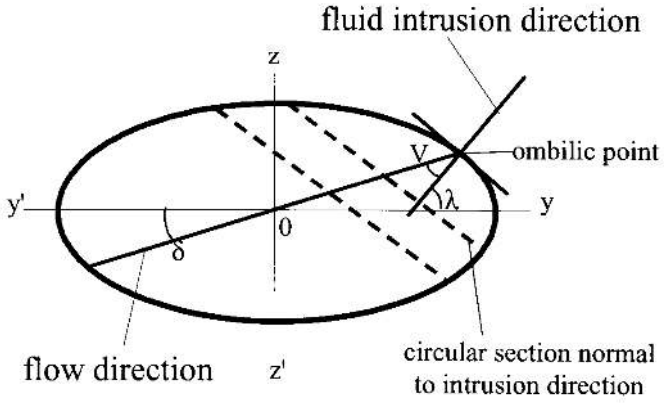

Figure 1. Representation of the equivalent pore model [7].

The tortuosity factor is then calculated from equation (v).

$$t_z^2 = \sqrt{1+\left(\frac{1}{c/a}\right)^2} \qquad (v)$$

Image analysis

The use of image analysis provides accurate local variations in the radial and longitudinal structural properties, such as porosity and mean pore size.

This technique is based on the consolidation of the porous structure by the use of a resin (araldite CY212), which fills the porous space of the fibrous medium. In order not to modify noticeably the porous structure, the fibrous sample and the resin were degassed separately until a low-vacuum was reached. Then, the resin was poured into the crucible containing the sample and atmospheric pressure was slowly reached to allow the slow percolation of the resin into the pores. Next, using a rotary microtome and polishing disks (from 60 to 0.25 μm paper grades), longitudinal or transversal slices of consolidated samples were obtained for Scanning Electron Microscope (SEM) observations using backscattered electron imaging at a magnification of 450 times in order to discriminate pores and fibres. The grey level images were binarized using a mean square criteria algorithm for thresholding [15] so as to separate fibres from pores. The binarized images were then analysed using Visilog software in order to measure stereological parameters [16,12].

Stereological analysis provides the secant number in the fibres per unit of measured length (N_L, mm^{-1}) and the total surface area of the pores per unit of measured surface area (A_A, mm^2/mm^2). These two stereological parameters are determined from images of cross-sections x0z and x0y and for each of the layers constituting the fibrous medium, called *upstream*, *centre* and *downstream* respectively as shown in Figure 2 [6]. The number of images analysed was chosen so as to reach 2 % precision for the intercept number measurements and 0.2 % for the pore surface area respectively, which corresponds to approximately 40 images and a surface area of 1 mm^2 according to the sample.

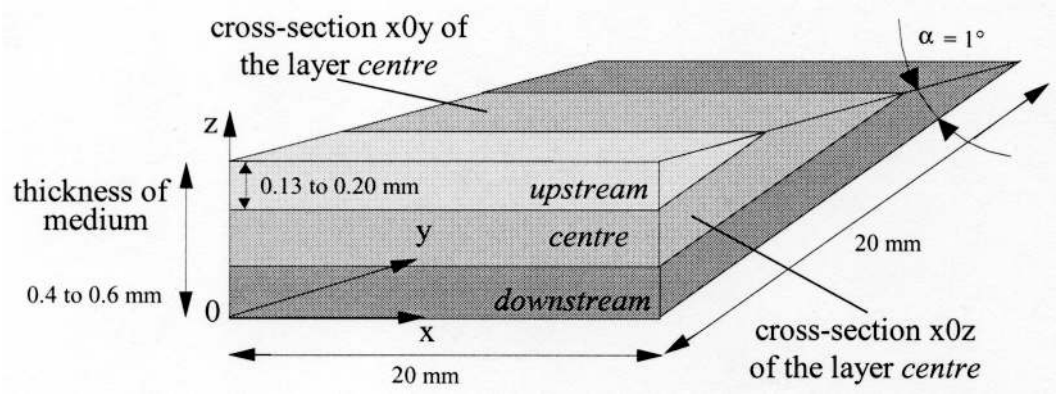

Figure 2. Schematic view of consolidated sample slices.

The stereological analysis was performed considering different viewing angles of the cross-section observed, from 0 to 180 ° and every 15 °, in order to access the structure anisotropy and to estimate the tortuosity factor (eq. v) of the porous path according to the "equivalent pore" model [7].

The structural parameters of porous media are calculated from the stereological analysis and the equivalent pore approach as follows:

$$\varepsilon = \frac{\text{volume des pores}}{\text{volume total}} = A_A \qquad \text{(vi)}$$

$$S_V = 4 <N_L> \qquad \text{(vii)}$$

$$<\phi> = \frac{4\,A_A}{S_v} = \frac{A_A}{<N_L>} \qquad \text{(viii)}$$

where $c / a = \frac{N_{Lx}}{N_{Lz}}$

Estimation of permeability

The permeability coefficient (B, m^2) can be deduced from the above structural parameters considering equation (ix) [17]. This permeability coefficient represents an intrinsic property of the porous media.

$$B = \frac{\varepsilon\,(<\phi>/4)^2}{2t_z^2} = \frac{\varepsilon^3}{2t_z^2\,S_v^2} \qquad \text{(ix)}$$

RESULTS AND DISCUSSION

Structural Parameters

The overall structural parameters of the unstrained fibrous media are measured using mercury porosimetry and image analysis techniques. Local structural parameters are also obtained from stereological analysis of the three layers constituting the media (see Figure 2). Moreover, mercury porosimetry is used to characterize the influence of medium deformation, when submitted to pressure drop, on the modification of structural parameters.

Unstrained fibrous media

The characterization of structural parameters from mercury porosimetry and stereological analysis is presented in Table 2 for media not submitted to the action of any friction forces.

From mercury intrusion volume curves and applying equation (iii), two characteristic pore size distributions can be distinguished for all the fibrous media, as shown in Figure 3a for the *33% 0.6 + 67% 2.7* medium. The wider pore size distribution corresponds to the roughness of the fibrous media and represents pores located on the upstream and downstream surfaces of the media. The distribution of smaller pores characterizes the internal porous structure inside the medium thickness.

Table 2 shows good adequacy between the mean hydraulic diameters and porosity measured by the two methods. The results indicate the influence of fibrous composition on the structural parameters of the paper. Indeed, for the same mean fibre diameter, fibre length exhibits a significant influence on porous structure comparing data obtained for the *100% 2.7 – L = 0.3 mm* and *100% 2.7 – L = 0.9 mm* media. Porosity and hydraulic pore diameter increase with fibre length whereas media made of a blend of the two fibre lengths, *100% 2.7 furnished*, leads to an intermediate porous structure. Considering the influence of fibre diameter on structural parameters, the two media made of one set of fibres (*100% 0.6* and *100% 2.7 µm furnished*) present a decrease in hydraulic pore diameter with decreasing mean fibre diameter. This result is consistent with the

Table 2. Structural parameters and permeability coefficients deduced from mercury porosimetry and image analysis for unstrained fibrous media.

Fibrous media	Mercury porosimetry				Image analysis			
	ε	$<\phi>$ (μm) eq. (i)	t_z^2 eq. (iv)	B $.10^{-12}$ (m^2) eq. (ix)	ε eq. (vi)	$<\phi>$ (μm) eq. (viii)	t_z^2 eq. (vi)	B $.10^{-12}$ (m^2) eq. (ix)
100% 0.6	0.926	7	2.2	0.6				
33% 0.6 + 67% 2.7	0.910	10	2.7	1.1	0.916	13	1.9	2.5
100% 2.7 furnished	0.930	25	2.4	7.6				
100% 2.7 – L=0.3 mm	0.925	22	2.1	6.7	0.925	24	1.8	9.2
100% 2.7 – L=0.9 mm	0.936	28	2.8	8.2	0.939	28	2.1	11.0
67% 0.6 + 33% 6	0.917	8	2.4	0.8				
50% 0.6 + 50% 6	0.920	12	2.4	1.7	0.912	18	2.0	4.6
33% 0.6 + 67% 6	0.921	14	3	1.9				

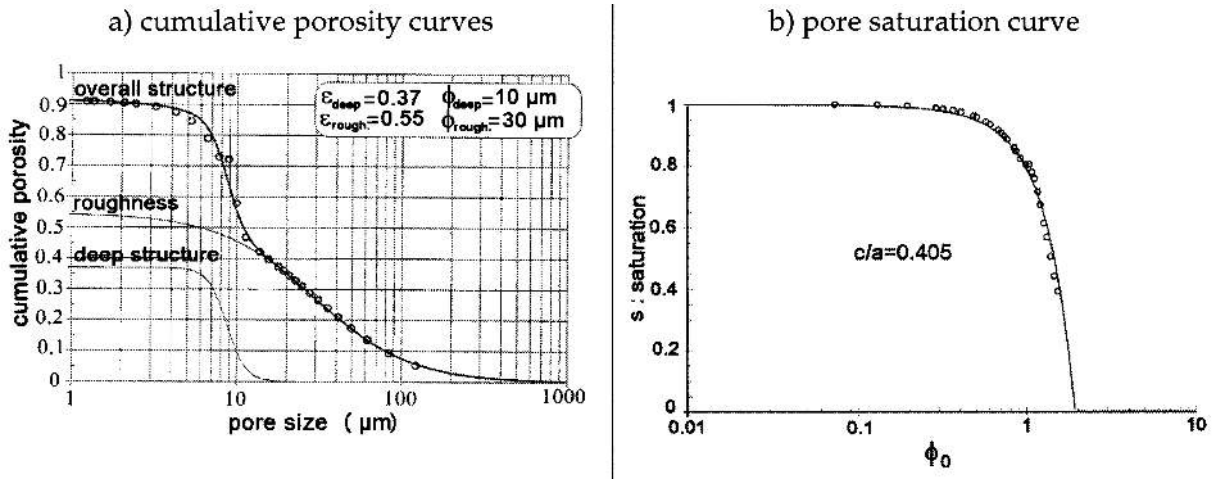

Figure 3. Cumulative porosity and saturation curves deduced from mercury porosimetry experiments for the medium *33% 0.6 + 67% 2.7*.

hydraulic diameter definition given by equation (i), which is related to the specific surface area of fibre. Moreover, for the three fibrous media composed of two fibre types in different proportions, 0.6 and 6 μm diameters, their structural properties decrease with the increasing mass fraction of the finest fibres.

The tortuosity factors (t^2_z) show the same variation with fibrous composition considering the two measurement methods. Nevertheless, image analysis techniques lead to significantly lower tortuosity factors than mercury porosimetry ones. This can be explained by the fact that the ellipticity coefficient (c/a) is deduced from intercept measurements on the whole thickness of the media for stereological analysis whereas it is obtained from internal pore size distribution for the mercury porosimetry technique (Figure 3b). So, in the first case, it represents the tortuosity factor obtained in the thickness of the overall porous structure (internal and roughness) while in the porosimetry case, it deals only with the internal structure of the media.

The permeability coefficients (B) calculated from equation (ix), using structural parameters deduced from mercury porosimetry and image analysis characterizations, are presented in Table 2. In Figure 4, these permeability coefficients are compared with those deduced from permeametry experiments. A good agreement is found between permeability calculated from mercury porosimetry

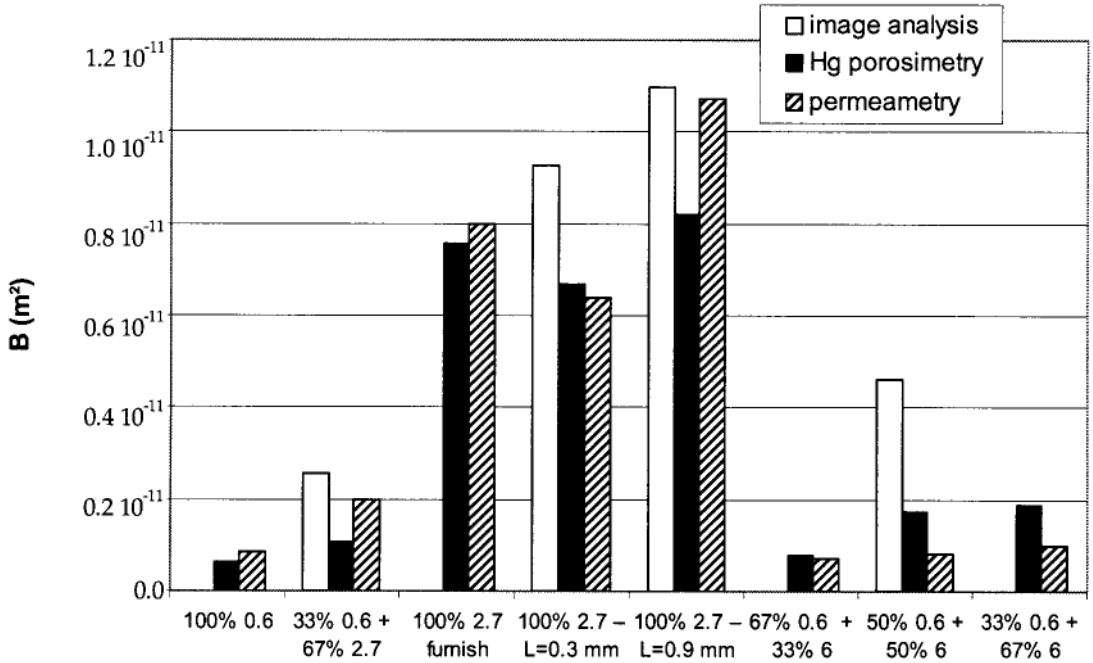

Figure 4. Permeability coefficients obtained from equation (ix) from mercury porosimetry and image analysis experiments: comparison with air permeametry measurements.

tests and permeability related to pressure drop measurements for air flow through the medium based on Darcy's law (see equation (x)). The permeability coefficients estimated using data from image analysis characterization are overestimated compared with pressure drop measurements. This tends to indicate that structural parameters deduced from the mercury porosimetry technique using the "pore equivalent" model are representative of the porosity, the mean hydraulic diameter and the tortuosity factor participating in air flow. So, the average structural parameters governing air flow traversing fibrous media are those of the internal structure while fibrous media roughness does not seem to have a major impact on media permeability.

$$B = \frac{e\,\eta\,\langle v\rangle}{\Delta P} \qquad (x)$$

Figure 5 presents the influence of the sheet formation process on structural parameters at different levels in the thickness of three studied media. Pore size and porosity gradients can be observed between the upstream and the downstream layer and are sharper for the *33% 0.6 + 67% 2.7* medium than for the *100% 2.7* samples. This can be explained by the fact that, during fibre filtration on the forming fabric, fibres of smaller diameter and length percolate through the fibre cake and concentrate in the downstream side of the medium (sieved by the forming fabric). In the case of *100% 2.7* samples, diameter and length dispersions are weak, resulting in a slight pore gradient. In contrast, for a blend of two different fibre compositions (mean diameters of 0.6 and 2.7 μm), characteristic dimension dispersions are significant and lead to a fibre composition gradient in the medium thickness.

Moreover, the two *100% 2.7* media exhibit similar mean pore sizes, which is in agreement with the fact that medium pore size mainly depends on fibre diameter.

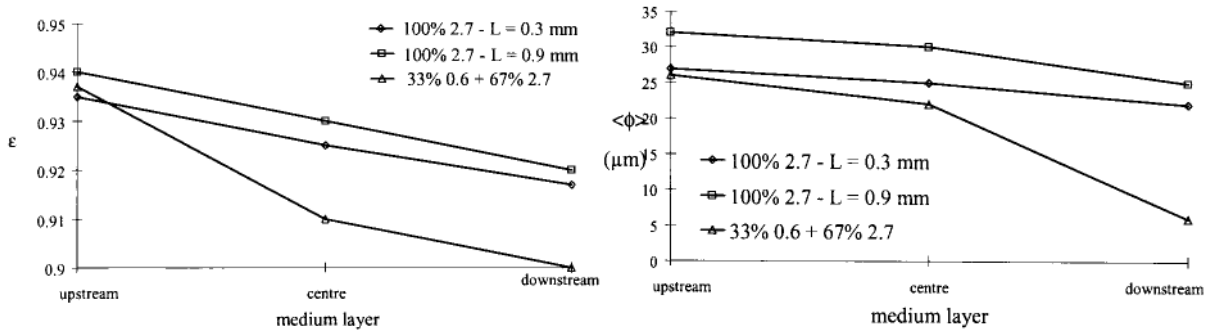

Figure 5. Porosity and pore hydraulic diameter measured from stereological analysis at the three levels in the thickness of three media.

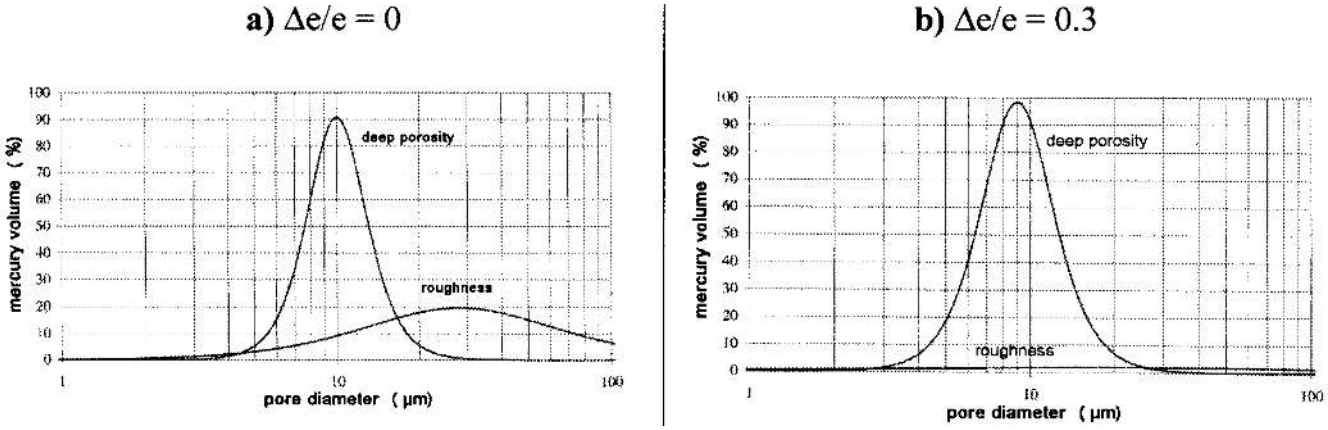

Figure 6. Differential porosity curves deduced from mercury porosimetry experiments: influence of strain (Δe/e) on the porous structure of the *33% 0.6 + 67% 2.7* medium.

Compression influence on media structure

In order to evaluate the influence of medium compression, when submitted to pressure drops generated by fluid flow through a porous structure, some mercury porosimetry measurements were performed on compressed media. Table 3 presents the variations in structural parameters and permeability coefficients for different applied pressures. The relative variation in thickness ($\Delta e/e$) resulting from applied pressure is also reported in Table 3. The corresponding permeability coefficients are deduced from equation (ix) and from permeametry measurements (equation x).

A good agreement between the two permeability coefficients (when permeametry measurements are available) is observed. This tends to validate the estimation of structural parameters from the "equivalent pore" model applied to the mercury porosimetry technique developed in the present study for compressed media. Moreover, the structural parameters obtained indicate that the relative variation in medium thickness is a result of a modification of internal structural parameters. Indeed, Table 3 shows a significant decrease in porosity and pore size values and a large increase in the tortuosity factor following an increase in medium deformation.

Considering that the range of pressures studied is of the same order of magnitude as pressure drops experienced by fibrous media during liquid filtration, the results obtained indicate that porous medium deformation must be considered for filtration optimization or prediction [11].

CONCLUSIONS

Stereological analysis is of interest to measure local structural parameters when porous media present a porosity and/or pore size gradient. The results obtained using this image analysis technique on anisotropic fibrous media show the same variation as structural parameters deduced from mercury porosimetry data post-processed by means of the "pore equivalent" model. Nevertheless, stereological analysis leads to overestimated structural parameters compared with mercury porosimetry. This is mainly due to the fact that mercury porosimetry data are post-processed to exclude media roughness information (which is not of interest for media permeability prediction) while image analysis data are not.

Permeability coefficients calculated from structural parameters deduced from mercury porosimetry experiments are in good agreement with those obtained from permeametry measurements for unstrained media as well as for compressed media. This can be explained by the major influence of the internal porous structure of media on flow behaviour through porous media.

Finally, a pore size distribution model has been developed to predict mercury porosimetry data. This can be used to quantify the major influence on structural parameters of fibrous media deformation when submitted to flow.

NOMENCLATURE

d	fibre diameter, μm
e	thickness, μm
s	pore volume saturation
v	superficial velocity of fluid, m s^{-1}
t^2_z	tortuosity factor along the medium thickness
A_A	total surface area of pores per unit of measured surface area
B	permeability coefficient, m^2
L	fibre length, mm
N_{Li}	secant number per unit of measured length in the i direction, mm^{-1}

Table 3. Structural parameters and permeability coefficients deduced from mercury porosimetry and permeametry for fibrous media under pressure.

Media	ΔP (10^5 Pa)	$\Delta e/e$	Mercury porosimetry e	<ϕ> (μm)	T^2_z	B $.10^{-12}$ (m^2)	Permeametry B $.10^{-12}$ (m^2)
	0	0	0.93	10	2.7	1.1	1.4
33% 0.6	0.18	0.15	0.89	8.2	4.0	0.47	0.49
+ 67% 2.7	0.53	0.30	0.86	7.6	4.7	0.33	0.37
	1.42	0.45	0.83	4.9	6.1	0.10	
	0	0	0.94	28	2.8	8.2	10.0
100% 2.7	0.14	0.15	0.92	17.0	4.1	2.0	2.1
L = 0.9 mm	0.27	0.25	0.89	16.5	5.5	1.4	
	0.80	0.45	0.86	16.0	41.6	0.17	

$<N_L>$	mean secant number per unit of measured length (mean value for all directions of plane), mm^{-1}
P	probability distribution of porosity versus pore size
W	specific weight, g m^{-2}
S_v	specific surface area per unit of volume, m^{-1}
α_i	slope attenuation coefficient
$<\phi>$	mean hydraulic pore diameter, μm
ϕ_i^{mod}	modal hydraulic pore diameter of pore size distribution i, μm
ϕ_0	dimensionless hydraulic pore diameter
η	dynamic viscosity, Pa s
ε	porosity
ε_i^{max}	overall porosity of pore size distribution i
c/a	ellipticity coefficient
ΔP	pressure drop, Pa

REFERENCES

1. Cushman, J., Theory and Applications of Transport in Porous Media - The Physics of fluids in hierarchical Porous Media: Angstroms to Miles, Kluwer Academic Publishers, Dordrecht, The Netherlands. (1997).
2. Kfoury, M., Ababou, R., Noetinger, B. and Quintard, M., Upscaling fractured heterogeneous media: Permeability and mass exchange coefficient, *J. Appl. Mech.-Trans. ASME*, **73**, 41-46 (2006).
3. Holmstad, R., Antoine, C., Nygard, P. and Helle, T., Quantification of the three-dimensional paper structure: Methods and potential, Pulp & Paper-Canada, **104**, 47-50 (2003).
4. Silvy, J., The paper and its unsuspected dimensions, *Mate. Sci. Forum*, **455-456**. 781-786 (2004).
5. Giesche, H., Mercury porosimetry: A general (practical) overview, *Particle & Particle Systems Characterization*, **23**, 9-19 (2006).
6. Le Coq L. and Montillet A., Characteristics of fixed-beds packed with anisotropic particles – Use of image analysis, *Powder Technol*., **121**, 138-148 (2001).
7. Silvy, J., La transformation conforme du pore équivalent, méthode d'homogénéisation de la texture des milieux polyphasés, *Récents Progrès en Génie des Procédés* - Tec & Doc Lavoisier, **3**, 484-493 (1989).
8. Paulapuro, H., Papermaking Part 1: Stock preparation and wet end In: *Papermaking Sci. Technology*, Fapet Oy Publisher, Helsinki, Finland (2000).
9. Huber P., Roux J.-C., Mauret E., Belgacem N. and Pierre C., Suspension crowding for a general fiber length distribution: application to flocculation of mixtures of short and long papermaking fibres, *J. Pulp Paper Sci*., **29**, 77 (2003).
10. White, C.F., Wet formed non-woven webs from high performance fibres, *Tappi J*., **72**, (12), 109-118 (1989).
11. Le Coq L., and Silvy, J., Fibrous media plugging modelling for liquid filtration, *Chem. Eng. Comm*., **174**, 145-166 (1999).
12. Montillet, A. and Le Coq, L., Image analysis: A useful tool for porous media characterization, *Chem. Eng. Technol*., **26**, 1285-1289 (2003).
13. Washburn, E.W., The dynamics of capillary flow, *Phys. Rev*., **17**, 273–283 (1921).
14. Benesse, M., Le Coq, L. and Solliec, C., Study of particle capture mechanisms in woven activated carbon filters: image analysis, In: World Filtration Congress, New Orleans, LA, USA, 18-24 April, American Filtration and Separation Society : Richfield MN, USA (2004).
15. Otsu N., An automatic threshold selection method based on discriminant and least square criteria, *Trans. IECE*, **63**, 349-356 (1980).
16. Underwood, E.E., *Quantitative Stereology*, Addison Wesley, Reading, Ma, USA (1970).
17. Carman, P. C., *The Flow of Gases in Porous Media*, Butterworths Scientific Publications, London (1956).